

Electrically Conductive Silicone Nano-Composites For Stretchable RF Devices

J. Agar¹, J. Durden¹, D. Staiculescu¹, R. Zhang¹, E. Gebara², C.P. Wong¹

¹*School of Materials Science and Engineering, Georgia Institute of Technology, Atlanta, GA*

²*School of Electrical and Computer Engineering, Georgia Institute of Technology, Atlanta, GA*

Abstract — The objective of this paper is to show how stretchable conductive composites can be utilized for the fabrication of ultra-low cost stretchable RF devices. We show a method to produce biocompatible highly conductive stretchable silicone composites via an *in-situ* nanoparticle formation and sintering process. Furthermore, we develop a simple, low cost, processing technique to fabricate stretchable RF transmission lines. These RF transmission lines are highly flexible, stretchable and robust. The S-parameter measurements show stable performance during mechanical deformation up to 6 GHz. Future development of this technology will enable ultra low cost consumer RF devices serving as a platform for future stretchable electronic devices.

Index Terms — Nano-Composites, Flexible, Stretchable, Biocompatible Electronics.

I. INTRODUCTION

The possibility of incorporating new functionality by designing flexible and stretchable electronic devices has captured the interest of engineers. Rapidly growing fields like radio frequency identification (RFID), wireless body area networks (WBAN), and medical implantable devices often require robustness, flexibility, stretchability, biocompatibility, comfort, and most importantly, ease of manufacturing and low cost.

These stretchable electronic devices require natural integration at the system, device and package level in the form of a functional package. The flexible and stretchable package has to enable natural integration with its environment and its movements. New flexible and stretchable fabrication processes and interconnection technologies must be developed, focusing on simplicity of design and functionality. Recent technological successes have been able to fabricate functional flexible electronics, however have all failed to develop a package capable of meeting the stringent requirements for biocompatibility, comfort and reliability for low cost consumer RF devices.

Previous work by Rogers et al. [1] summarizes several novel methods to fabricate stretchable devices based on mechanically wavy structures. Their approach utilizes materials that are not intrinsically stretchable or flexible. Instead, Rogers et al. utilizes ultra thin wavy interconnects to minimize compressive and tensile stresses that occur during bending and stretching [1]. Although novel in approach, the techniques necessary for fabrication are too complex and expensive for ultra-low cost consumer electronics.

One approach to fabricate stretchable devices utilizing intrinsically stretchable electrically active components was reported by Hu et al. [2]. They used single wall carbon

nanotube (SWCNT) networks dispersed in a gel and printed on a rubber substrate. Conduction within the composite was achieved through the formation of a percolated network of SWCNT. These composite materials are highly stretchable and remain conductive even after tensile strains of 700% [2]. However, these stretchable conductors were permanently deformed and damaged after stretching [3]. A second problem with stretchable SWCNT conductors is the high resistivity of the composite ($\sim 1 \times 10^{-2} \Omega \text{ cm}$), which limits their application in electronic devices.

A third approach to produce stretchable RF antennas utilized a liquid metal (Gallium Indium (GaIn) Eutectic) as a stretchable conductor. It has been shown that using this approach it is possible to produce stretchable half wave dipole antennas and inverted cone antennas [4-6]. This approach to fabricate stretchable RF devices is low cost and highly scalable. However, stretchable liquid metal RF devices have a few practical problems that prohibit their use in consumer electronics. First, indium resources are scarce, thus the already high price of indium is highly influenced by changes in demand. Secondly, GaIn eutectic like other heavy metals is toxic, prohibiting their use in any wearable application. Most importantly, GaIn eutectics have a melting point of 10.2°C. This temperature is well above the minimum operational temperature required for consumer electronics.

We show, for the first time, a biocompatible, intrinsically stretchable flexible conductive nano-composite designed into a stretchable microstrip line with good performance up to 6 GHz. The high performance of our conductive composite material results from the addition of a chemical additive that causes the formation and sintering of nanoparticles on the surface of the silver conductive fillers within the composite. Our approach is novel in its simplicity, enabling rapid prototyping and fabrication in a bench-top environment. Furthermore, our fabrication scheme requires minimal capital investment; the only equipment needed is a spin coater and a microstencil. The ultra-low cost fabrication process makes technology transfer simple and scalable. The materials and fabrication techniques developed in this paper present a process for fabrication of new stretchable RF devices for novel applications including antennas for curvilinear spaces [7] and reconfigurable antennas [8].

II. MATERIALS AND METHODS

A. Preparation of Stretchable Conductive Composite

Electrically conductive composites (ECC) were fabricated using silicones containing a bimodal distribution of silver flakes ranging in size from 1 μm to 20 μm (Ferro Corporation). Silver flakes were dispersed in the silicone matrix formulation in an 80:20 (wt%/wt%) ratio. For the conductive composites treated with additive A, the mixture was 80:18:2 (wt%/wt%/wt%) of silver flakes, silicone and additive A respectively. The electrical resistivity of silicone ECC was measured using a Keithley 2000 multimeter. Morphological changes in silver flakes resulting from treatment with additive A were determined by treating silver flakes with additive A at 150 °C for 15 min. Characterization of the resulting particle morphology was imaged using a LEO 1530 Scanning Electron Microscope (Carl Zeiss).

B. Fabrication of Microstrip Line

Polymethylmethacrylate (PMMA) dissolved in anisole was spin coated onto a bare silicon wafer. 1.5 mm wide lines of uncured conductive composite were stencil printed using a flip-up microstencil (Mini Micro Stencil Inc.). The composite used for the ground plane was screen-printed between two pieces of Kapton tape 8 mils thick. The conductive composite was cured at 150°C for 30 min. Following curing of the conductive composite, uncured degassed silicone was poured on top of the Si wafer and was allowed to cure at room temperature for 24 hrs. The thickness of the silicone encapsulation was controlled by weight. The PMMA was dissolved in acetone and the silicone encapsulated conductive composite was removed from the Si wafer using a razor blade. The conductive lines were cut using a razor blade and bonded to a stretchable ground plane using a small amount of uncured silicone. The ground plane was fabricated in a process identical to the microstrip line. After curing for 24 hrs, excess silicone was cut using a razor blade and the final microstrip line was obtained. The fabrication process for the microstrip line is shown in Fig. 1.

C. Preparation of Tensile Specimen

The ECC material was prepared in a strip by stencil printing the ECC between two pieces of Kapton tape. Following encapsulation and lift off as described in section B, dog bone shaped tensile specimens were cut using a razor blade, in accordance with ASTM D412. The electrical response under tensile elongation was measured using a Keithley 2000 and an Instron 5548 microtester. Resistance values were recorded at 0.25 second intervals during tensile elongation to 30% at an extension rate of 10 mm/sec. Repeat testing of the electromechanical of the tensile specimens to tensile elongations of 30% response was conducted. Finally, the electromechanical response of the dog bone samples were measured until failure under tensile load.

D. Microwave Characterization

The microstrip line S-parameters from 100 MHz to 6 GHz were measured with a E8364B PNA Network Analyzer using a SOLT calibration. Connection to the measurement system was established using 18 GHz SMA connectors. These connectors were chosen because they matched perfectly to the dimension of the microstrip line and no soldering was necessary. The lines were tested in multiple geometrical configurations.

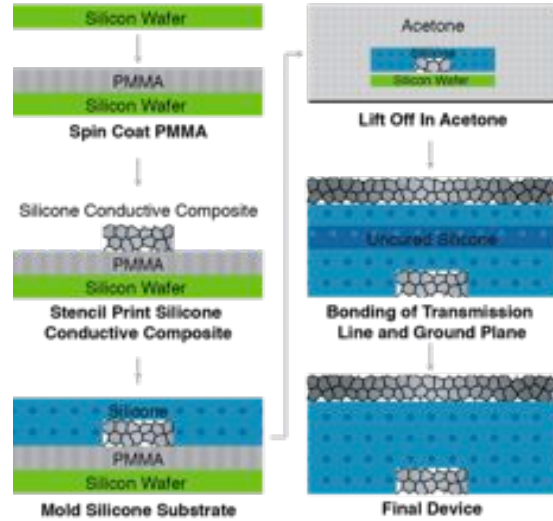


Fig. 1. Schematic drawing of microstrip line fabrication process.

III. MATERIALS CHARACTERIZATION

A. Characterization of Electrically Conductive Composites

Silicone ECC test strips were prepared as described in Section II-A. Following curing the ECC undergoes a transition from insulating to conductive. However, ECCs formulated without additive A had high resistivity. Many composites formulated without additive A were insulating. The high resistance and inconsistent results using untreated silicone ECC limits its application in RF devices. However, silicone ECC formed with additive A had a much lower resistivity ($\sim 2 \times 10^{-4} \Omega \text{ cm}$). Additive A functions by reducing the silver carboxylate on the surface of the silver flakes. The reduction of silver carboxylate has two active roles. First, the reduction process removes stearic acid surfactants. These surfactants are necessary for proper dispersion and to prevent aggregation of the silver flakes during mixing. However, these surfactants also limit the intimate contact between conductive fillers. Secondly, the reduction process forms small nano/submicron-sized particles on the surface of the silver flakes. These *in-situ* formed nano/submicron sized particles on the surface of the silver flakes have high surface area to volume ratios and are not stabilized by surfactants. Thus these *in-situ* formed particles are less thermodynamically stable. The thermodynamic instability of these *in-situ* formed particles causes the particles to sinter at low temperatures ($\sim 150^\circ\text{C}$).

The sintering process reduces or eliminates contact resistance between flakes, enhancing the conductivity and reliability of the ECC. The effect of the addition of additive A on the morphology of the silver flakes can be seen in Fig. 2. What is important to notice in the untreated silver flakes (Fig. 2A) is that the surface is smooth and the flakes appear to be stacked one on top of another. However, in the treated sample (Fig. 2B) the silver flakes have a higher surface roughness. Also, large flakes appear to be connected by small branching arms. This branching process resulting from the sintering of *in-situ* formed nanoparticles results in dramatically improved reliability and conductivity of the composite material.

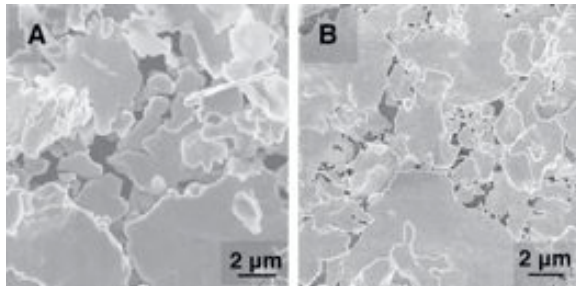


Fig. 2. A. SEM image of untreated Ag flakes showing smooth surface morphology. B. SEM image of additive treated Ag flakes. Surface of Ag flakes shows rough morphology with evident sintering of *in-situ* formed Ag nanoparticles.

It is worth emphasizing that it is essential that these nanoparticles are formed *in-situ* and not just added to the formulation. The addition of pre-formed nanoparticles to composite formulations requires the nanoparticles to be stabilized with a surfactant to prevent aggregation during processing. These surfactants on pre-formed nanoparticles stabilize the surface, reducing the driving force for sintering. Thus, conductive composites formed with pre-formed nanoparticle fillers typically have higher resistivity due to reduced contact area and thus increased contact resistance.

B. Characterization of Stretchability

Simultaneous tensile and electrical resistance measurements were measured as described in Section II B. The results from these experiments are shown in Fig. 3. During the first trial the resistance of the ECC remained relatively constant up to tensile strains of $\epsilon = 0.3$. However, following the first tensile experiment, the tensile strain caused the anisotropic silver flakes to align. The strain induced reorganization caused the resistance of the composite to increase. However, subsequent tensile strains of $\epsilon = 0.30$ had no additional effect on the resistance. Tensile-electrical measurements of the pre-strain dog bone specimen during strain to failure showed the resistance of the ECC initially decreased and then increased until finally failing at a strain of $\epsilon = 0.70$.

C. Microwave Measurements

The transmission line was measured in three different configurations: straight, bent and twisted. The result in Fig. 4 shows little to no difference between these three conformations, indicating that the line performance is unaltered by the bending and twisting of the line.

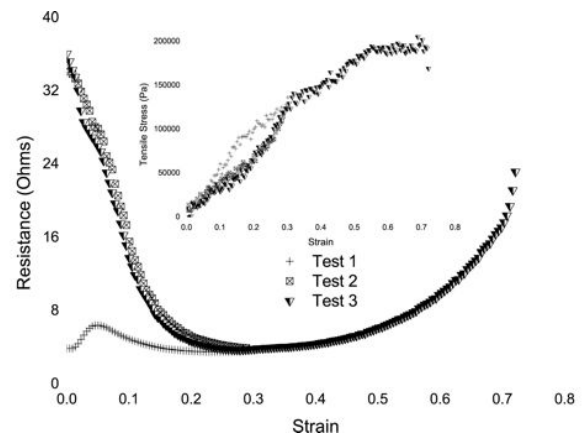


Fig. 3. Simultaneous tensile electromechanical characterization of silicone ECC. Inset: stress strain curve of dog bone tensile specimen.

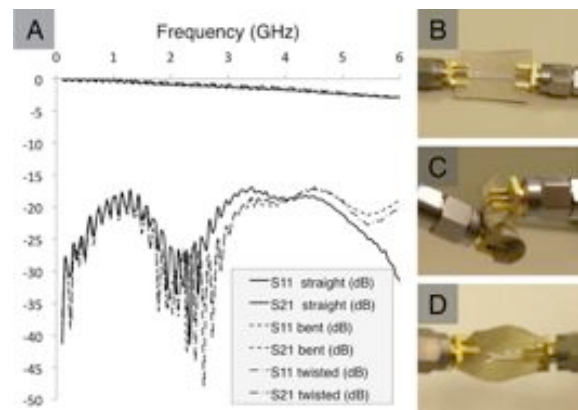


Fig. 4. A. S-parameter measurement results for different line configurations: B. Straight C. Bent D. Twisted.

The measured insertion loss at 6 GHz was found to be ~ 3 dB. However, full wave measurements in High Frequency Structure Simulator (HFSS) using the extracted DC resistivity of $2 \times 10^{-4} \Omega \text{ cm}$ showed a much lower insertion loss, of about 0.5 dB at 6 GHz. This discrepancy between the simulated and experimental results can be attributed to two key factors. First, the resistivity is expected to increase with frequency and the simulator only used the measured DC conductivity. The second, more important reason for this discrepancy is due to the poor contact between the SMA connector and the microstrip line. Hence the actual S-parameters of the transmission line are expected to be better than measured and closer to the simulated values. The poor contact resistance is likely due to the small contact area between the signal pin connector and the microstrip signal line. The poor contact between the SMA connectors and the microstrip line was

verified using the Keithley 2000 multimeter. The DC resistance of the bare signal line was measured to be $0.2\ \Omega$. Measuring the resistance through the SMA contacts resulted in a total resistance of $5\ \Omega$. This high contact resistance results in parasitic mismatch, translating in increased losses during RF measurement.

Due to the poor mechanical contact of the connector we were unable to quantify the changes in S-parameters with lengthwise stretching of the line. However, data from the simultaneous tensile DC testing (Fig. 3) promises good and predictable results in the RF regime during tensile elongations.

Following RF testing, cross sections of the formed microstrip lines were imaged using a 3D confocal microscope (Olympus Corporation). An image of a cross section is shown in Fig. 5.



Fig. 5. Cross-section of the microstrip line.

Fig. 6 shows the stretchability and flexibility of our composite material that has been optimized for improved mechanical properties. The improved mechanical properties of this line results from the improved adhesion at the conductive composite silicone interface. Improved adhesion enhances load distribution through the conductive composite during stretching, reducing the probability of failure. The highly elastomeric nature of the composite material enables tensile strains of 100% to be accommodated without any plastic deformation or damage to the device. Future development of this technology and processes will enable more complex and stretchable RF devices to be fabricated. Furthermore, development of new materials and processes will enable active components to be incorporated on this stretchable flexible platform.

IV. CONCLUSION

We show for the first time, a biocompatible, intrinsically stretchable flexible conductive nano-composite material designed into a stretchable microstrip line with good performance up to 6 GHz. The high performance of our conductive composite results from the addition of a chemical additive that causes the formation and sintering of nanoparticles on the surface of silver conductive fillers within the composite. Our approach is novel in its simplicity enabling rapid prototyping and fabrication in a bench-top environment,

requiring only minimal capital investment. The ultra-low cost fabrication process makes technology transfer simple and scalable. Future development of this technology will enable ultra low cost consumer RF devices as well as serve as a platform for future stretchable electronic devices.

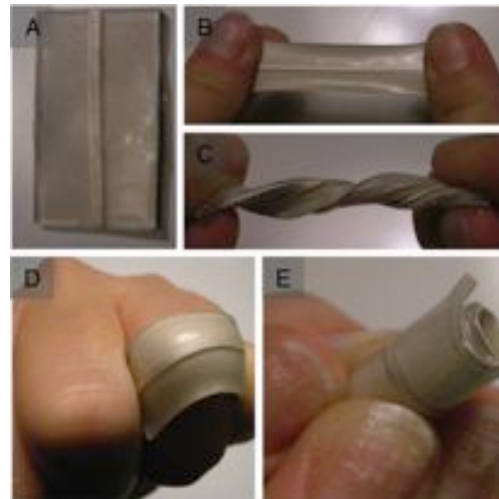


Fig. 6. Improved mechanical properties in action: A. Unstretched. B. 100% stretch. C. 720° twist. D. Bent around a curvilinear body shape. E. Rolled.

REFERENCES

- [1] J. Rogers, T. Someya, Y. Huang, "Materials and Mechanics for Stretchable Electronics", *Science*, 2010, 327, pp. 1603-1607.
- [2] L. Hu, W. Yuan, P. Brochu, G. Gruner, Q. Pei, "Highly stretchable, conductive, and transparent nanotube thin films," *Applied Physics Letters*, vol. 94, p. 161108.
- [3] T. Sekitani, T. Someya, "Stretchable, Large-area organic electronics", *Advanced Materials*, 2010, 22, pp. 2228-2246.
- [4] J-H. So, J. Thelen, A. Qusba, G.J. Hayes, G. Lazzi, M.D. Dickey, "Reversibly Deformable and Mechanically Tunable Fluidic Antennas", *Advanced Functional Materials*, 2009, 19, 3632-3637.
- [5] S. Cheng, Z. Wu, P. Hallbjörner, K. Hjort, A. Rydberg, "Foldable and Stretchable Liquid Metal Planar Inverted Cone Antenna", *IEEE Trans. Antenna and Propagation*, Vol. 57, No. 12, Dec 2009, 3765-3771.
- [6] M. Kubo, X. Li, C. Kim, M. Hashimoto, B.J. Wiley, D. Ham, G.M. Whitesides, "Stretchable Microfluidic Radiofrequency Antennas", *Advanced Materials*, 2010, 22, pp. 2749-2752.
- [7] N. Tiercelin, P. Coquet, R. Sauleau, V. Senez, H. Fujita, "Polydimethylsiloxane membranes for millimeter-wave planar ultra flexible antennas", *J. Micromech. Microeng.*, 16, pp. 2389.
- [8] N. Kingsley, D.E. Anagnostou, M. Tentzeris, J. Papapolymerou, "RF MEMS Sequentially Reconfigurable Sierpinski Antenna on a Flexible Organic Substrate With Novel DC-Biasing Technique", *Journal of Microelectromechanical Systems*, Vol. 16, No 5, October 2007, pp. 1185-1192.
- [9] S. Xu, B.J. Hansen, Z.L Wang, Piezoelectric-nanowire-enabled power source for driving wireless microelectronics", *Nature communications*, 19 October 2010.